Highlights

A Home Energy Management System Incorporating Data-Driven Uncertainty-Aware User Preference

Yinyan Liu,Jin Ma,Xinjie Xing,Xinglu Liu,Wei Wang

- A cost-effective home energy management system is proposed incorporating data-driven user preference.
- Development of a non-intrusive load monitoring (NILM) algorithm for the uncertainty of load consumption results.
- Preference level is quantitatively defined with NILM results for load scheduling and responding DR signals.
- Uncertainties related to preference level are used in the multi-objective decision-making process.

A Home Energy Management System Incorporating Data-Driven Uncertainty-Aware User Preference

Yinyan Liu[a], Jin Ma[a,*], Xinjie Xing[b], Xinglu Liu[c] and Wei Wang[d]

[a]The University of Sydney, J03 Electrical & Information Engineering Building, Sydney, 2006, New South Wales, Australia

[b]The University of Liverpool, Management School, Liverpool, L69 3BX, England

[c]Tsinghua University, Tsinghua Berkeley Shenzhen Institution, Intelligent Transportation and Logistics Systems Laboratory, Guangdong, Shenzhen, 518055, China

[d]Hong Kong University of Science and Technology, Data Science and Anaytics, Information Hub, HKUST (Guangzhou), Guangzhou, 511458, China

ARTICLE INFO

Keywords:
Non-intrusive load monitoring,
Bayesian neural network,
Uncertainty Aware,
user preference,
home energy management system

ABSTRACT

Today, with the increase in the integration of renewable sources, the home energy management system (HEMS) has become a promising approach to improve grid energy efficiency and relieve network stress. Traditionally, complicated thermal models or passive participation of the users prevents HEMS from fully automating the involvement of demand-side energy management. In this paper, an advanced HEMS is proposed incorporating uncertainty-aware user preference. The energy consumption user behavior, including temporal and temperature habits, is firstly characterized in a data-driven way with non-intrusive load monitoring (NILM). To capture the potential uncertainties resulting from the characteristics of NILM modeling, a novel NILM model is developed with Bayesian theory. The NILM-based preference level is further integrated into the HEMS to schedule the appliances and respond the demand response (DR) signals for economic benefits. Extensive experiments are performed with the real-world dataset. The effectiveness and superiority of the proposed algorithm are demonstrated particularly in reducing the energy cost, maintaining the user's preference level, and encouraging users to participate in DR. Compared to a traditional HEMS as a benchmark, the proposed HEMS for a 24-hour horizon can trade-off limited electricity costs to keep the preference at a high level.

1. Introduction

Energy management is a crucial matter all around the globe. Considering that 27% of global energy consumption and 17% of CO_2 emissions are generated from residential energy consumption, a robust energy efficiency strategy in the residential sector should be developed [1]. To achieve decarbonization and respond to global climate change, clean energy transitions through utilizing more and more renewable energy sources (RES), such as solar photovoltaic (PV) and wind, are underway. Today the expansion of distributed energy resources and the phaseout of the feed-in tariff scheme make residential users, especially the users with renewable resources (all known as prosumers), move from passively consuming electricity to actively participating in demand response (DR) or demand management [2]. Self-consumption and electricity sharing with a community of consumers/prosumers are becoming more popular and profitable [3]. With the development of innovative information and communication technologies, understanding energy consumption behavior for residential users is of paramount importance for the design of new energy management strategies [4].

[⋆] This work is supported in part by the Australia-China Science and Research Fund Joint Research Center for Energy Informatics and Demand Response Technologies, and in part by Australian Research Council (ARC) under Grant A Unified Framework for Resource Management in Edge-Cloud Data Centers (DP200103494), and in part by UK-Australia Centre in a Secure Internet of Energy: Supporting Electric Vehicle Infrastructure at the "Edge" of the Grid, EP/W003325/1.

[*]Corresponding author E-mail address: j.ma@sydney.edu.au (J. Ma)

Recent developments in smart meters and wireless communication, along with the instruction of smart home appliances (i.e., air conditioning, washing machine, dishwasher, etc.), have made it possible for a fully automated home energy management system with assessing household characteristics and behaviors in electricity consumption. Advanced HEMS requires monitoring and controlling energy generation and consumption for economic or environmental optimization, taking into account energy consumption behavioral habits. Accordingly, many studies have been dedicated to HEMS in the last decade [5, 6].

1.1. Literature review for HEMS

HEMS plays an essential role in DR to provide financial benefits for energy efficiency [7]. Traditionally, demand-side management (DSM) was utility-driven. Still, with an increase in the integration of renewable sources, it also becomes a "consumer-driven" process, and the HEMS becomes more and more essential for the demand side [8]. On the one hand, the end-use consumers seek to optimize their energy resources through HEMS. HEMS provides decision support for residential users to effectively and automatically schedule home energy resources. By acting as a delegation of the user to communicate with the utility and grid, HEMS can help the user participate in the smart grid. On the other hand, the utility seeks to improve the grid operational efficiency by coordinating many residential HEMSs with schedulable appliances such as heating, ventilation, and air conditioning (HVAC) [9].

From the utility's perspective, a two-stage coordinating scheme between multiple HEMSs and the utility has been modeled [10] to reduce the peak demand and minimize the power losses. The utility communicated and aggregated each bus's load consumption and PV outputs to decide each customer's required peak reduction values [11]. With a hierarchical incentive-based DR strategy, the utility can send appropriate DR signals to the potential DR participants [12]. To decrease the demand-side peak-to-average ratio and maximize the energy profit of the utility, a model-free reinforcement learning technique has been applied for intelligent multi-microgrid energy management [13]. Recent years, reinforcement learning-based HEMS has received a lot of attention from researchers [14, 15]. Reinforcement learning (RL) can be used to solve very complex problems for real-time energy management. However, RL-based HEMS requires a good, comprehensive and representative set of training data that covers all the situations which a HEMS needs to handle, which is very difficult in real applications. If the training set is inadequate, which happens quite often in real world, the performance of RL-based HEMS algorithms will be downgraded. Either the traditional optimization-based or the RL-based HEMS algorithms, they are designed from the utility's viewpoint which rarely considers the user's willingness and energy consumption preference. How to characterize and modeling the user's energy behavior preference in the energy management system is critical to the success of DSM. It hinges heavily on the consumers' participation levels in DR programs.

Existing research focused on the user's perspective mainly minimizes the electricity cost and the end-user discomfort. Complicated thermal models and temperature deviations are often used to define the discomfort function for appliances scheduling in a home [16, 17]. For instance, a thermal dynamics model was adopted in [18] to restrict the indoor temperature within a comfortable range. Besides, some studies also model the personalized temperature discomfort profiles and deviations of appliances' operation time through surveys or user's manual settings [19, 20, 21]. However, due to the complexity of the thermal models and the lack of personalized features, both the theoretical modeling and the survey methods have difficulties collecting effective and accurate parameters/feedback. Consequently, it limits HEMS applications in smart grids on a large scale. Meanwhile, the personalized energy consumption behavior is related to the preferred temperature and also significantly affected by the preferred running time of the appliances [22].How to automatically understand the time and temperature preferences of the user's energy consumption habits and apply them to HEMS has not yet been studied.

1.2. Literature review for user behavior

For advanced HEMS, it is difficult to reduce the energy use or energy consumption cost without understanding users' behavior and preference. Many studies have investigated user energy consumption preference based on three methods: 1) choice experiments, 2) users' feedback, and 3) mathematical models. In choice experiments, participants are asked to choose their preferred temperature constraints manually [19, 20]. Users' feedback is mainly used to evaluate the satisfactory level rather than define the user behavior preference. Euclidean distance between the actual consumption and the target consumption has been adopted to assess the satisfactory level for pricing and energy-efficiency problems [23]. For energy-saving recommendations, users' feedback also can be used as prior knowledge about users' habits [24]. In addition to evaluating satisfactory level, users' feedback can also be directly integrated into the control logic [25] or provide real-time electricity consumption information [26] for home energy management.

User's participation is required for both the choice experiments and users' feedback, deviating from the 'automatic' and 'smart' design for home energy management. Mathematical models that quantify the user preference level for home appliance scheduling should be developed. Two approaches are usually used to quantify the user preference level: 1) manual comfort constraint setting and 2) historical data-based preference calculation. Many studies developed different thermal models by manually setting minimum and maximum temperature constraints. For example, the authors in [27] developed preference levels based on the indoor temperature. In contrast, floor temperature and hot-water temperature are controlled in a comfort range in [28].

With the enormous amounts of data produced every day by sub-meters and smart sensors installed in residential buildings, more and more historical data-based user behavior models have been proposed. To quantify the user's comfort, the moment the user frequently/sometimes/rarely uses the electric appliances has been calculated and defined by a cluster method according to the historical data in [29]. The authors in [30] calculate the user preference vector with the appliance's ON/OFF frequency, which is obtained by non-intrusive load monitoring or sub-meter data. A qualitative method based on visual thermal landscaping is proposed in [31] to investigate the patterns of users' thermal preferences and enhance user comfort and energy performance. Personal comfort has been quantitatively analyzed with individual differences and spatial context information.

The mathematical model for understanding user behavior is the ideal choice. However, existing studies for mathematical models either need to set preferred temperature manually with only thermal comfort considered or focus only the frequency of the use of the electric appliances. To better characterize users' energy consumption behavior, the appliances' preferred operation time and temperature should be considered jointly to develop the comfort or preference model. Although the HEMS has been extensively researched, less research pays attention to an automatic user energy consumption behavior interpretation to support a personalized definition of preference. NILM is a promising choice to understand user energy consumption behavior by monitoring household appliances in a cost-effective, fully automatic, and non-intrusive way.

1.3. Literature review for NILM

If leveraged properly, the data produced every day can be used for understanding user's habits, which can aid in better energy management to reduce wasted energy and promote sustainable and energy-efficient behavior [32]. NILM can be treated as a blind source separation problem, which tries to estimate energy consumption of appliances from aggregated load [33]. With the robust learning and characteristic expression abilities of deep learning, more and more deep learning-based methods have shown their advantages when applied for NILM [34, 35]. The authors in [36] demonstrated that combining the data augmentation and teacher-student network can efficiently improve the feature representation capability of their model with unlabeled data. To address the simultaneous action problems under real-time NILM framework, a three-stage algorithm is proposed in [37] with event detection, deep dictionary learning, and sparse coding formalized algorithm.

Generally, residential appliances are divided into schedulable that can be shifted or non-schedulable that must operate immediately with the user's request [38, 39]. Non-schedulable appliances such as lighting systems, kettles, and computers must operate immediately at the request of the user, while the operation time of the schedulable appliances such as air conditioning can be shifted according to the electricity price or the requirement of the DR. The HVAC contributes more than 30% of the total electricity consumption [40]. A time-frequency mask-based decomposition approach has been proposed in [41] to extract flexible loads of HVAC and lighting contributions. A recent review work of fault detection and efficiency assessment for HVAC using NILM can be found in [42]. However, the NILM-based schedulings for the HVAC have not been comprehensively studied in HEMS so far.

1.4. Literature review of NILM-based HEMS

Understanding the energy consumption habits of the consumer with NILM can make the HEMS become a "consumer-specific" system in a natural automatic way. A NILM-based HEMS has been studied in [43] with the k-nearest neighbor method and genetic algorithm. A multi-task learning-based NILM has been developed for a microgrid energy management system by regarding the operation time deviation of the schedulable appliances as a comfort level metric[39]. Recently, Cimen et al. proposed an online energy management system for AC/DC residential microgrids with NILM [44]. The average consumption, the average operation time (OT), the average number of daily uses (NU), and the most preferred operation interval (POI) have been defined with NILM results as the user behavior for energy management optimization.

In all the existing NILM-based HEMS, only the time/frequency of the appliances' use is considered as the user behavior. However, if we want to understand and maximize the user's preference in HEMS, both the preferred time and temperature should be understood from the NILM results. Besides, home energy management is a decision-making problem. The optimization algorithm should consider the uncertainty of the user's preference obtained from the NILM results. Developing an algorithm for NILM to obtain the uncertainty for further scheduling rather than only point estimates of the disaggregations has not been studied.

1.5. Approach and contributions

According to the above literature review, there are three issues needed to be addressed for advanced HEMS: (i) How to understand and quantitatively define the user energy consumption behavior in a fully automated way; (ii) How to obtain the uncertainty of the NILM results for further HEMS; (iii) How to design multi-objective HEMS with the uncertainty NILM results to minimize user's energy cost and maximize user's preference level. Therefore, this paper proposes a NILM-supported home energy management system with uncertainty-aware user preference. The Bayesian neural network (BNN) is adopted in our proposed NILM model to achieve load monitoring and quantify the level of uncertainty for the NILM results. Then, a novel user behavior characterization and the corresponding preference level are quantitatively defined upon the NILM results. The proposed preference level includes the appliances' preferred time/frequency use and the comfort temperature use of the air conditioning. To trade off the energy consumption cost against the preference level, the user behavior is integrated into the HEMS for optimized scheduling. The significant contributions of this paper are three-fold:

1) A Bayesian neural network-enabled NILM model is established to obtain the uncertainty score of the NILM results rather than only the point estimates of the ground truth. The on/off state of the schedulable appliances can be obtained with uncertainty score for further HEMS.
2) Quantitative user behavior characterization, including the operation time and temperature, is defined based on the NILM results and the uncertainty score. The user's behavioral effect is further modeled to design HEMS with consideration of the user's preference level and user's willingness to participate in DR.
3) A multi-objective HEMS that minimizes the costs and maximizes the user's preference level considering the uncertainty of the NILM results is developed. This is the first work to invest the practical application of NILM in HEMS, which is treated as a multi-objective optimization problem considering the uncertainty of NILM results. The effectiveness of the proposed algorithm is evaluated with real-world dataset for both the prosumer with PV and consumer without any renewable resources.

2. Uncertainty-Aware User Preference

To obtain the uncertainty score of the NILM, a Bayesian neural network that models all the weights with probability distributions rather than a single fixed value is firstly designed in this section. Furthermore, most of existing research only defines user behavior with the preferred operation time from NILM [39, 43]. However, other quantitative features derived from NILM results, such as operating temperature, are essential for various schedulable appliances in user behavior characterization. So, the quantitative user behavior characterization considering both the time and temperature usage of appliances are defined with NILM results. Finally, two parameters that reflect the degree of user preference for use time/frequency $\zeta_{i,t}^{time}$ and comfort temperature $\zeta_{i,t}^{temp}$ are calculated with uncertainty. The overall proposed algorithms for uncertainty-aware NILM and preference level calculation are shown in Fig. 1. Since the on-state events are relatively rare for some appliances [34], such as a washing machine, keeping the ratio of off- and on-state samples are applied as data pre-precessing for the imbalance problem. Then, a BNN-based model is proposed for energy disaggregation to obtain the energy consumption of electric appliances and the corresponding estimation uncertainty. Furthermore, quantitative user behavior is characterized by NILM results. Last, preference level considering the preferred operation time and temperature can be calculated for further optimization of HEMS.

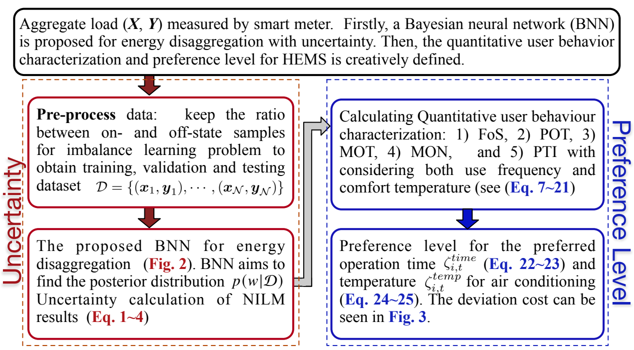

Figure 1: The overall framework for uncertainty-aware NILM and preference level calculation.

2.1. Bayesian Neural Networks-Enabled NILM

NILM can monitor energy consumption behavior of some specific appliances from the whole power consumption of a household. Suppose that there are N electrical appliances in a house, NILM tries to disaggregate the power consumption of the ith appliance $\boldsymbol{y}^i \in \mathbb{R}^{T_y} = (y_1^i, \dots, y_{T_y}^i)$ from the total power consumption $\boldsymbol{x} \in \mathbb{R}^L = (x_1, \dots, x_L)$ for time $\mathcal{L} = [1, \dots, L]$, where the output length T_y of $\boldsymbol{y}^i$ is usually less than the input length L [45]. With N number of appliances in a house, there is $x_t = \sum_{i=1}^{N} y_t^i + \epsilon_t$, where ϵ_t is the noise factor [33]. A large number of neural network-based algorithms have been applied to the NILM and are superior to traditional algorithms, such as the Hidden Markov model (HMM) [34, 39, 46].

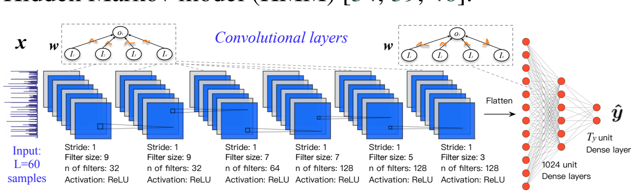

Figure 2: The framework of Bayesian neural network-based NILM

All of the neural networks-based NILM only provide the point estimates of the predictions and do not accurately represent the uncertainty inherent with the prediction, which is critical to further scheduling or decision making. To understand users' energy consumption behavior and to obtain the uncertainty sore of the personalized preference level for HEMS, a BNN-enabled NILM is inspired by the Bayesian neural network approach in [47]. In particular, it represents all the weight in the neural network with probability distributions over possible values rather than having a single fixed value of deep neural networks (DNN). As shown in Fig. 2, we apply Bayesian to the convolutional neural network (CNN) for NILM [48].

Given a training dataset $\mathcal{D} = \{(\boldsymbol{x}_i, \boldsymbol{y}_i)\}_{i=1}^{\mathcal{N}} \subset \mathcal{X} \times \mathcal{Y}$, where $\mathcal{X}$ is the set of total power in a residential household and $\mathcal{Y}$ is the set of the corresponding labels, BNN aims to find the posterior distribution $p(w|\mathcal{D})$ over model parameters $\boldsymbol{w}$ based on Bayes' theorem [49],

$$p(\boldsymbol{w}|\mathcal{D}) = \frac{p(\mathcal{D}|\boldsymbol{w})p(\boldsymbol{w})}{p(\mathcal{D})} \tag{1}$$

where $p(\mathcal{D}|\boldsymbol{w})$ is the likelihood, $p(\mathcal{D})$ is the marginal likelihood, and $p(\boldsymbol{w})$ is the prior. Variational approximation can be applied to find an approximated distribution $q(\boldsymbol{w}|\theta)$ parameterized over θ by minimizing the Kullback-Leibler (KL) divergence of $q(\boldsymbol{w}|\theta)$ and $p(\boldsymbol{w}|\mathcal{D})$,

$$\begin{aligned} \theta^\star &= \arg\min_\theta \mathrm{KL}[q(\boldsymbol{w}|\theta)||p(\boldsymbol{w}|\mathcal{D})] \\ &= \arg\min_\theta \int q(\boldsymbol{w}|\theta) \log \frac{q(\boldsymbol{w}|\theta)}{p(\mathcal{D}|\boldsymbol{w})p(\boldsymbol{w})} \mathrm{d}\boldsymbol{w} \\ &= \arg\min_\theta \mathrm{KL}[q(\boldsymbol{w}|\theta)||p(\boldsymbol{w})] - \mathbb{E}_{q(\boldsymbol{w}|\theta)}[\log p(\mathcal{D}|\boldsymbol{w})] \end{aligned} \tag{2}$$

where $\mathrm{KL}[q(\boldsymbol{w}|\theta)||p(\boldsymbol{w})]$ is the KL divergence of the variational posterior distribution $q(\boldsymbol{w}|\theta)$ and the prior $p(\boldsymbol{w})$, $\mathbb{E}_{q(\boldsymbol{w}|\theta)}[\log p(\mathcal{D}|\boldsymbol{w})]$ is the likelihood cost that related to the training dataset $\mathcal{D}$. To further minimize the cost with gradient descent, unbiased Monte Carlo sampling can be applied to evaluate the expectations in Equation (2),

$$\begin{aligned} \mathcal{F}(\mathcal{D}, \theta) &= \mathrm{KL}[q(\boldsymbol{w}|\theta)||p(\boldsymbol{w})] - \mathbb{E}_{q(\boldsymbol{w}|\theta)}[\log p(\mathcal{D}|\boldsymbol{w})] \\ &\approx \sum_{i=1}^{n} \log q(\boldsymbol{w}^i|\theta) - \log p(\boldsymbol{w}^i) - \log p(\mathcal{D}|\boldsymbol{w}^i) \end{aligned} \tag{3}$$

where $\boldsymbol{w}^i$ is the ith Monte Carlo sample drawn from the variational posterior $q(\boldsymbol{w}^i|\theta)$. Considering that the training process of neural networks always adopts mini-batch gradient descent [50], Equation (3) can be rewritten as,

$$\begin{aligned} &\mathcal{F}(\mathcal{D}, \theta) = \sum_{i=1}^{M} \mathcal{F}_i(\mathcal{D}_i, \theta) \\ &\approx \sum_{i=1}^{M} \frac{1}{M} \left[\mathrm{KL}[q(\boldsymbol{w}|\theta)||p(\boldsymbol{w})] - \mathbb{E}_{q(\boldsymbol{w}|\theta)}[\log p(\mathcal{D}|\boldsymbol{w})] \right] \end{aligned} \tag{4}$$

where M is the total mini-batch in the training dataset, each gradient is averaged over all elements in one minibatch. A probability distribution of the weights can be trained for the NILM model with variational learning and Monte Carlo. The disaggregation results of schedulable appliance $i \in \mathcal{I} = [1, \dots, I]$ are just a possible sample of the model, and the uncertainty score $u_{i,t}^{nilm}$ of the NILM results for ith schedulable appliance at time t can be calculated as the standard deviation of the mean of multiple samples,

$$u_{i,t}^{nilm} = \sqrt{\frac{\sum(\hat{y}_{i,t} - \mu)^2}{n(n-1)}}, \ \forall i \in \mathcal{I}, \ \forall t \in \mathcal{L} \tag{5}$$

where $\hat{y}_{i,t}$ is the disaggregation results with the BNN-NILM and μ is the mean value for n samples from the BNN-based NILM. With the energy consumption estimation, the *on/off* states $\hat{s}_{i,t}$ of the ith appliance can be obtained with a threshold ξ_i,

$$\hat{s}_{i,t} = \begin{cases} 1, & \hat{y}_{i,t} \geq \xi_i, \ \forall i \in \mathcal{I}, \ \forall t \in \mathcal{L} \\ 0, & \hat{y}_{i,t} < \xi_i, \ \forall i \in \mathcal{I}, \ \forall t \in \mathcal{L} \end{cases} \tag{6}$$

2.2. Quantitative User Behavior Characterization

To maximize user's preference in the HEMS, the user behavior traits should be firstly characterized. In particular, those traits related to the difference between non-schedulable and schedulable appliances are elaborately incorporated. In this work, quantitative user behavior characterization is creatively designed with the energy disaggregation results in K-day historical data. Let $t \in \mathcal{T} = [1, \ldots, T]$ as the scheduling time slot in a day and T_r represents the time steps of NILM results in each $t \in \mathcal{T}$ scheduling time slot. There are $T \times T_r$ NILM results in a day. Accordingly, we consider five attributes, namely (i) frequency of use [22], (ii) preferred operation time (*POT*), (iii) maximum operation time (*MOT*), (iv) maximum operation number (*MON*), and (v) preferred temperature interval (*PTI*) for the operation of the air conditioning, which is sensitive to the temperature.

1) Frequency of the Use: Firstly the frequency of the appliance's *on* state (FoS) is defined here as a quantitative index on the user's power consumption behavior,

$$FoS_{i,t} = \frac{\sum_{k=1}^{K} \sum_{tr=1}^{T_r} \hat{s}_{i,k,t}^{tr}}{K}, \ \forall i \in \mathcal{I}, \ \forall t \in \mathcal{T} \tag{7}$$

However, FoS does not consider user's tendency to regularly use the appliance. The regular high frequency of usage for a appliance means that the user's preference for the appliance has a certain degree of regularity [22]. Therefore, the regular frequency of use (RFoU) is quantified as follow,

$$\begin{aligned} RFoU_{i,t}^{start} &= \frac{\sum_{k=1}^{K} Ns_{i,k,t}}{K}, \quad RFoU_{i,t}^{end} = \frac{\sum_{k=1}^{K} Ne_{i,k,t}}{K} \\ RFoU_{i,t}^{dur} &= \frac{\sum_{k=1}^{K} Nd_{i,k,t}}{K}, \quad RFoU_{i,t}^{on} = \frac{\sum_{k=1}^{K} Non_{i,k,t}}{K} \end{aligned} \tag{8}$$

$$Ns_{i,k,t} = \begin{cases} 1, & \text{if } (\hat{s}_{i,k,t}^{tr-1} = 0) \& (\hat{s}_{i,k,t}^{tr} = 1) \\ & \to tr \in [2, T_r], \& (\sum_{t'=tr}^{T_r} \hat{s}_{i,k,t}^{t'} = T_r - tr) \\ 0, & \text{otherwise.} \end{cases} \tag{9}$$

$$Ne_{i,k,t} = \begin{cases} 1, & \text{if } (\sum_{t'=1}^{tr} \hat{s}_{i,k,t}^{t'} = tr) \& (\hat{s}_{i,k,t}^{tr} = 0) \\ 0, & \text{otherwise}, \forall tr \in [1, T_r]. \end{cases} \tag{10}$$

$$Nd_{i,k,t} = \sum_{tr=2}^{T_r} \mathbb{J}(\hat{s}_{i,k,t}^{tr})$$

$$\mathbb{J}(\hat{s}_{i,k,t}^{tr}) = \begin{cases} 1, & \text{if } (\hat{s}_{i,k,t}^{tr-1} = 0) \& (\hat{s}_{i,k,t}^{tr} = 1) \\ & \& (\hat{s}_{i,k,t}^{T_r} = 0) \\ 0, & \text{otherwise}, \forall tr \in [2, T_r]. \end{cases} \tag{11}$$

where $Ns_{i,k,t}$, $Ne_{i,k,t}$, and $Nd_{i,k,t}$ calculate the operation number of the ith appliance that starts to work, turn off, and complete a work cycle during the tth time slot. If the appliance keeps at *on* during the tth time slot, namely $\sum_{tr=1}^{T_r} \hat{s}_{i,k,t}^{tr} = T_r$, there is $Non_{i,k,t} = 1$, else $Non_{i,k,t} = 0$.

$$RFoU_{i,t} = RFoU_{i,t}^{start} + RFoU_{i,t}^{end} + RFoU_{i,t}^{dur} + RFoU_{i,t}^{on} \tag{12}$$

A larger $RFoU_{i,t}$ means that the user prefers to use the ith appliance in the tth time period.

2) Preferred Operation Time (POT): Understanding the POT of the user can help HEMS schedule the appliances in different time slots with the user's preference in mind. According to $FoS_{i,t}$ and $RFoU_{i,t}$, we define POT as,

$$\begin{aligned} v_{i,t} &= (FoS_{i,t} + RFoU_{i,t})/2 \\ POT_i &= [t \text{ for } t \in [1, \ldots, T], \ \ v_{i,t} \geq \xi_{pot}] \end{aligned} \tag{13}$$

where ξ_{pot} is the weight for the POT definition.

3) Maximum Operation Time: HEMS needs to schedule the operation time of an appliance less than its extended maximum operation time,

$$OT_i^{max} = \max [OT_1, \ldots, OT_{mt}, \ldots, OT_{Mt}] \tag{14}$$

$$OT_{mt} = \bar{t}_2 - \bar{t}_1 \tag{15}$$

$$\text{where } \ \bar{t}_1, \bar{t}_2 \in [1, T_r \times T]$$

$$\bar{t}_1, \bar{t}_2 \ s.t.$$

$$(\hat{s}_{i,\bar{t}_1} = 0) \ \& \ (\hat{s}_{i,\bar{t}_2} = 1) \& (\sum_{t'=\bar{t}_1}^{\bar{t}_2} |\hat{s}_{i,t'} - \hat{s}_{i,t'-1}| \leq 1) \tag{16}$$

OT_i^{max} is the maximum operation time of the ith appliance, OT_{mt} is the mtth operation time. There are totally Mt operations in the historical K days.

4) Maximum Operation Number: How many times the user prefers to use an appliance in one day is also chosen here as an index for understanding the user's behavior.

$$MON_i = \max [N_i^1, \ldots, N_i^k, \ldots, N_i^K] \tag{17}$$

where N_i^k is the operation number the ith appliance in the kth day.

5) Preferred Temperature Interval (PTI): The temperature concerned appliances such as air conditioning with high-power consumption play a vital role in the user's energy consumption. Generally, the user would like to operate the appliance when the temperature is too high or too low out of their comfortable zone. According to the *on/off* operation of the appliance and the outdoor temperature, the *PTI* can be defined as a metric for characterizing the user energy consumption behavior,

$$FoT_{i,\tau} = \frac{\sum_{k=1}^{K} \mathbb{I}(\hat{s}_{i,k,\bar{t}}, \tau_{\bar{t}})}{\sum_{k=1}^{K} \bar{\mathbb{I}}(\tau_{\bar{t}})}, \ \forall i \in \mathcal{I}, \forall \tau \in \mathcal{A} \tag{18}$$

$$\mathbb{I}(\hat{s}_{i,k,\bar{t}}, \tau_{\bar{t}}) = \begin{cases} 1, & \text{if } \hat{s}_{i,k,\bar{t}} = 1, \text{ and } \tau_{\bar{t}} = \tau \\ 0, & \text{otherwise}, \forall \bar{t} \in [1, T_r \times T]. \end{cases} \tag{19}$$

$$\bar{\mathbb{I}}(\tau_{\bar{t}}) = \begin{cases} 1, & \text{if } \tau_{\bar{t}} = \tau \\ 0, & \text{otherwise}, \forall \bar{t} \in [1, T_r \times T]. \end{cases} \tag{20}$$

$$PTI_i = \{\tau | FoT_{i,\tau} \geq \xi_{pti}, \forall i \in \mathcal{I}, \forall \tau \in \mathcal{A}\} \tag{21}$$

where $\tau \in \mathcal{A}$ is the outdoor temperature, $\mathcal{A}$ is the total different temperature during the K historical days, $FoT_{i,\tau}$ is the frequency operation of the ith appliance at temperature τ, and ξ_{pti} is the threshold to decide the preference temperature interval according to $FoT_{i,\tau}$.

2.3. Preference Level Definition

One of the main challenges for smart HEMS is how to minimize the user's comfort and habits disturbance caused in HEMS optimization through analysis of the user's power consumption preference. With the proposed BNN-enabled NILM, we can monitor the power consumption and *on/off* states of appliances, as well as quantify the user power consumption behavior with varying levels of uncertainties. In this work, the preference time level $\zeta_{i,t}^{time}$ and preference temperature level $\zeta_{i,t}^{temp}$ of the consumer are defined as follows,

$$\zeta_{i,t}^{time} = \begin{cases} 0, \ |t - T_i| \geq T_d^{time}, \ \ T_i \in \upsilon_{i,t} \\ \upsilon_{i,t}, \ 0 \leq |t - T_i| \leq T_d^{time}, \ T_i \in POT_i \\ 1, \ t \in \upsilon_{i,t} \end{cases} \quad (22)$$

$$\mathcal{P}_{i,t}^{time} = s_{i,t} \cdot \zeta_{i,t}^{time}, \ \forall i \in \mathcal{I}, \ \forall t \in \mathcal{T} \quad (23)$$

where $\upsilon_{i,t}$ is calculated with Equation (13), T_d^{time} is the tolerance time of deviation from preferred operation time, and $\zeta_{i,t}^{time}$ is obtained according to Fig.3 (a), $s_{i,t}$ is the scheduled *on/off* state of the ith appliance during time slot t in HEMS, and $\mathcal{P}_{i,t}^{time}$ indicates the preference time level of scheduling the ith appliance at time t in HEMS. Similarly, $\mathcal{P}_{i,t}^{temp}$ can be calculated with the capturing consumer's preferred temperature interval,

$$\zeta_{i,t}^{temp} = \begin{cases} 1, \ \ \tau_t \in PTI_i \\ FoT_{i,t}, 0 \leq |t - T_\tau| \leq T_d^{temp}, \tau \in PTI_i \\ 0, \ |t - T_\tau| \geq T_d^{temp}, \ \ \tau \in PTI_i \end{cases} \quad (24)$$

$$\mathcal{P}_{i,t}^{temp} = s_{i,t} \cdot \zeta_{i,t}^{temp}, \ \forall i \in \mathcal{I}, \ \forall t \in \mathcal{T} \quad (25)$$

where τ_t is the forecasting outdoor temperature at time t, T_τ is the time slot that is regarded as the preferred temperature interval, and T_d^{temp} is the tolerance time for deviation from preferred temperature interval. The calculation of $\zeta_{i,t}^{temp}$ is according to Fig.3 (b).

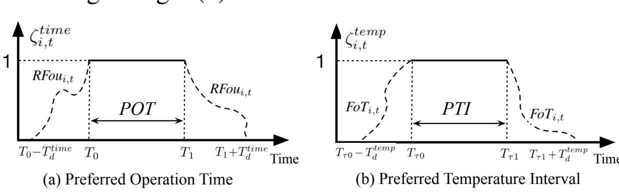

Figure 3: Deviation cost of preferred operation time and temperature interval

3. Proposed HEMS

The designed HEMS should perform optimal scheduling of the electrical appliances, the battery energy storage system (BESS), and the power exchanges with the external grid to minimize the energy cost and, at the same time, maximize the preference level of the user (see Fig. 4). With the total load measured by a smart meter, the energy consumption of concerned appliances can be monitored by the uncertainty indices based on the proposed NILM. Then, user habits can be quantitatively characterized as being presented in Section II. The HEMS can schedule the household appliances such as air conditioning and dryer according to the day-ahead electricity price and the user habits. Besides, we assume that the residential user can receive the DR signals during the peak time to earn revenue in the designed HEMS, making it easy to extend the proposed HEMS to a commercial user.

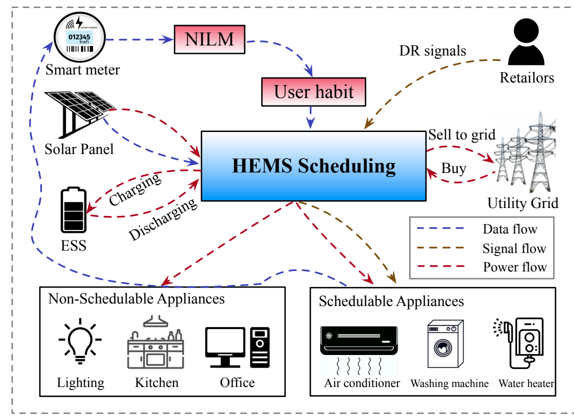

Figure 4: The structure of the proposed HEMS

3.1. Objective Functions of the HEMS

In this work, we design the HEMS by taking into account the power consumption cost, the income of selling power to the grid, the reward of responding to the DR signals in peak time, and the preference level considering the user's behavior pattern. Two different objectives, including energy cost and preference level for HEMS, are proposed.

1) Minimize Energy Cost: The HEMS seeks to minimize the total power cost, including buying power cost, selling power revenue, and DR reward, by determining the *on/off* states of schedulable appliances, power absorbing/feeding from/to the network over the horizon, energy storage charging/discharging, denoted as $\Xi = (\boldsymbol{s}, \boldsymbol{P}^{grid}, \boldsymbol{P}^{sell}, \boldsymbol{P}^{ch}, \boldsymbol{P}^{dis})$, respectively. Here $s_{i,t} \in \boldsymbol{s}$ is the *on/off* state of the ith schedulable appliance at time slot t. The objective function for power cost is formulated as follows,

$$\min_{\Xi} C = \sum_{t=1}^{T} (\lambda_t^{TOU} P_t^{grid} - \lambda_t^{SP} P_t^{sell} - \lambda_t^{dr} P_t^{dr}) \Delta t \quad (26)$$

where T is the time slots for HEMS scheduling in a day, Δt is the time resolution of a time slot, λ_t^{TOU} is the time of use pricing for electricity consumption, λ_t^{SP} is the spot price, P_t^{grid} and P_t^{sell} are the power bought from and sold to the utility grid at a given time t, respectively, P_t^{dr} is the electricity increase or decrease for responding to the DR event, and λ_t^{dr} is the DR reward of each kilowatt (kW).

2) Maximize Preference Level: HEMS and DR for appliance scheduling not only should minimize the energy cost but also should maximize the user's preference level according to their historical behavior or habit. In this work, we define the user's preference level ($\mathcal{P}$) by considering both preferred time and temperature based on the quantitative characterization of their behavior,

$$\max_{\Xi} \mathcal{P} = \sum_{t}^{T}\sum_{i}^{I}\left[(\mathcal{P}_{i,t}^{time} + \mathcal{P}_{i,t}^{temp})(1 - u_{i,t}^{nilm} s_{i,t})\right]$$
$$= \sum_{t}^{T}\sum_{i}^{I}\left[(s_{i,t}\cdot\zeta_{i,t}^{time} + s_{i,t}\cdot\zeta_{i,t}^{temp})(1 - u_{i,t}^{nilm} s_{i,t})\right] \tag{27}$$

where $\mathcal{P}_{i,t}^{time}$ and $\mathcal{P}_{i,t}^{temp}$ are the preference level of the user's preferred operation time and temperature at tth time slot, respectively, $u_{i,t}^{nilm}$ is the uncertainty score of the BNN-based NILM results for the ith appliance.

Following the discussion above, the objective function $\mathcal{B}$ of the designed HEMS can be formulated as follows,

$$\min_{\Xi} \mathcal{B} = f(\mathcal{C}, -\mathcal{P}) \tag{28}$$

Using the weighted sum method [51] to solve the multi-objective optimization problem in Eq. (28) entails selecting scalar weight ω and minimizing the following composite objective function:

$$\min_{\Xi} f(\mathcal{C}, -\mathcal{P}) =(1-\omega)\mathcal{C} + \omega(-\mathcal{P}) \tag{29}$$

$$=(1-\psi(\bar{u}))\mathcal{C} + \psi(\bar{u})(-\mathcal{P}) \tag{30}$$

where,

$$\psi(\bar{u}) =0.5(1-\bar{u}) \tag{31}$$

$$\bar{u} =\frac{\sum_{i}^{I}\sum_{t}^{T}(u_{i,t}^{nilm})}{(I+T)} \tag{32}$$

where $\bar{u}$ is the mean value of the uncertainties for the NILM results of the different appliances during the whole day. In this work, weight in the weighted sum method is the function of the uncertainty $\bar{u}$. According to Eq. (31), the weight will be 0.5 when $\bar{u} = 0$, where the actual load consumption is used for comparison with the NILM results. The introduction of uncertainty to the weight $\omega = \psi(\bar{u})$ means the larger the uncertainty of the NILM results, the less attention the objective will pay to the preference level.

3.2. DR Event Considering User Preference

For DR, one of the most essential and challenging problems is encouraging consumers to participate more actively in DR programs, especially during the peak time when high energy consumption and insufficient power generation take places. When the user's preferred behavior of using electrical appliances is not considered, a very low-level response to a DR event is normally yielded from this user. To encourage users to participate in DR actively, we creatively designed the user behavior effect into the DR event. The DR signal γ can require the user to increase ($\gamma = 1$) or decrease ($\gamma = -1$) the power consumption at peak time. The user's preference of starting to use and shutting off the ith appliance at the t time slot should be considered in HEMS for DR events. For example, if the user receives a DR signal $\gamma = 1$ and the power consumption of more than one appliance is close, the larger the $RFoU_{i,t}^{start}$, the more likely the ith appliance is scheduled to turn on for DR. Besides a fixed reward λ for each kilowatt response obtained from the utility, the effect of user behavior on the actual reward λ^{dr} is innovatively incorporated into the HEMS optimization model.

$$rfou_{i,t}^{start} = \begin{cases} 1, & RFoU_{i,t}^{start} \geq \xi_{sdr} \\ RFoU_{i,t}^{start}, & RFoU_{i,t}^{start} < \xi_{sdr} \end{cases} \tag{33}$$

$$rfou_{i,t}^{end} = \begin{cases} 1, & RFoU_{i,t}^{end} \geq \xi_{edr} \\ RFoU_{i,t}^{end}, & RFoU_{i,t}^{end} < \xi_{edr} \end{cases} \tag{34}$$

$$\lambda_{i,t}^{dr} = \begin{cases} \lambda(1-s_{i,t-1})\cdot s_{i,t}\cdot rfou_{i,t}^{start}, & \gamma = 1 \\ \lambda s_{i,t-1}\cdot(1-s_{i,t})\cdot rfou_{i,t}^{end}, & \gamma = -1 \\ 0, & \gamma = 0 \end{cases} \tag{35}$$

where ξ_{sdr} and ξ_{edr} are the tolerance thresholds for $RFoU_{i,t}^{start}$ and $RFoU_{i,t}^{end}$, respectively. So, the total DR reward at time t in Equation (26) can be refined as,

$$\lambda_{t}^{dr} P_{t}^{dr} = \sum_{i=1}^{I}(\lambda_{i,t}^{dr}\cdot P_{i,t}^{sc}\cdot|\gamma|), \forall t \in \mathcal{T} \tag{36}$$

where $P_{i,t}^{sc}$ is the active power consumption of the ith schedulable appliance in at time t. Note that, the actual energy operation cost C is calculated with fixed reward λ,

$$C = \sum_{t=1}^{T}(\lambda_{t}^{TOU} P_{t}^{grid} - \lambda_{t}^{SP} P_{t}^{sell} - \lambda P_{t}^{dr})\Delta t \tag{37}$$

The overview of the proposed algorithms is summarized in Fig. 5. The *on/off* states of the schedulable appliances and the preference level of time and temperature of NILM results are applied to update DR's reward. The task of HEMS is to schedule the usage of schedulable electric appliances to minimize the energy cost and maximize the preference level.

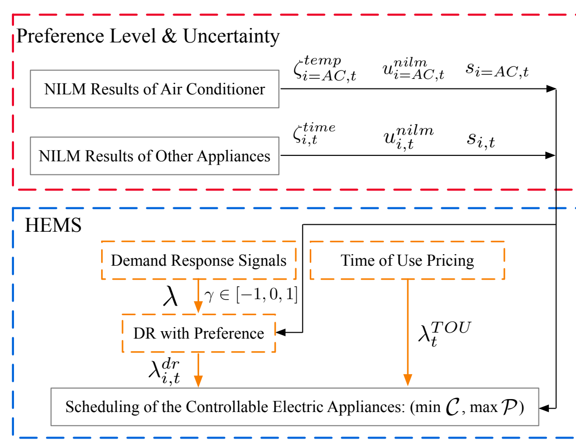

Figure 5: Overview of the proposed algorithm

3.3. Model Constraints

1) Home Energy Balance: The total energy demand of the household, including the energy consumption of the appliances and net generation to the grid, should be met by the power bought from the grid, the PV output, and power discharged from the BESS,

$$P_{t}^{grid} - P_{t}^{sell} + P_{t}^{pv} - P_{t}^{ch} + P_{t}^{dc} - P_{t}^{app} = 0, \ \forall t \in \mathcal{T} \tag{38}$$

$$P_{t}^{app} = \sum_{h=1}^{H_{ns}} P_{h,t}^{nsc} + \sum_{i=1}^{I} P_{i,t}^{sc}\cdot s_{i,t}, \ \forall t \in \mathcal{T} \tag{39}$$

$$0 \leq P_t^{sell} \leq (P_t^{pv} + P_t^{dc})(1 - \delta_t^{grid}),\ \forall t \in \mathcal{T} \quad (40)$$

$$0 \leq P_t^{grid} \leq P_{max}^{grid} \delta_t^{grid},\ \forall t \in \mathcal{T} \quad (41)$$

$$s_{i,t}, \delta_t^{grid} \in \{0, 1\},\ \forall i \in \mathcal{I},\ \forall t \in \mathcal{T} \quad (42)$$

where P_t^{pv} is the PV output, P_t^{ch} and P_t^{dc} are the charging and discharging power of the BESS, respectively. $P_{max,t}^{sell} = P_t^{pv} + P_t^{dc}$ is the maximum power the consumer can sell to the grid. It is limited by the PV output and the discharging power of the BESS. The power consumption of the appliances P_t^{app} includes the power consumption of non-schedulable appliances P_t^{nsc} and schedulable appliances P_t^{sc}. H and I are the number of non-schedulable and schedulable appliances in a household, respectively.

2) Battery Energy Storage System: For a prosumer with renewable generators, the BESS can provide reliable energy during a blackout or store excessive energy generated by renewables. It also provides the HEMS with a more flexible ability to sell the power to the grid. The charging and discharging of the BESS are modeled below,

$$SoC_{t+1} = SoC_t + (P_t^{ch}\eta_t^c - P_t^{dc}/\eta_t^{dc})\Delta t / E_{bess}^{max} \quad (43)$$

$$SoC^{min} \leq SoC_t \leq SoC^{max},\ \forall t \in \mathcal{T} \quad (44)$$

$$0 \leq P_t^{ch} \leq P_{ch,t}^{max} \delta_t^{ch},\ \forall t \in \mathcal{T} \quad (45)$$

$$0 \leq P_t^{dc} \leq P_{dc,t}^{max}(1 - \delta_t^{ch}),\ \forall t \in \mathcal{T} \quad (46)$$

$$\delta_t^{ch} \in \{0, 1\}, \forall t \in \mathcal{T} \quad (47)$$

where SoC_t, η_t^c, and η_t^c are the state-of-charge (SoC), the charging efficiency, and the discharging efficiency of the BESS at time t, respectively, E_{bess}^{max} is the maximum capacity of the BESS, SoC^{min} and SoC^{max} are the minimum and maximum SoC of the BESS, $P_{ch,t}^{max}$ and $P_{dc,t}^{max}$ are the maximum charging and discharging power, respectively, and δ_t^{ch} is a binary variable indicating that the BESS cannot be charging or discharging simultaneously [52].

3.4. Scheduling of Domestic Appliances

In this work, the designed HEMS optimizes the operation of the schedulable appliances such as air conditioning, washing machine, and water heater, and leaves the user to operate the non-schedulable appliances exactly as they wish. The scheduling of domestic appliances must be planned according to several operating parameters, such as the maximum operation time and maximum operation number,

$$\sum_{t=t_0}^{T_i^s+t_0} |s_{i,t+1} - s_{i,t}| \leq 2, \quad t_0 \in [1, \dots, T - T_i^s] \quad (48)$$

$$T_i^s = \begin{cases} 0, & MON_i \leq 1 \\ \lceil \dfrac{24}{\Delta t \cdot MON_i} \rceil, & MON_i > 1 \end{cases} \quad (49)$$

$$\sum_{t=t_0}^{T_i^s+t_0} (s_{i,t} * \Delta t) < \lceil OT_i^{max} \rceil, \quad t_0 \in [1, \dots, T - T_i^s] \quad (50)$$

where $\lceil \cdot \rceil$ is the operation of rounding up to the closest integer, and T_i^s is the interval time that the appliance can only operate once without the interruption. Equation (48) and Equation (49) keep the appliance from frequent operations, and Equation (50) makes sure that the operation time of the appliance is less than the maximum operation time OT_i^{max}.

4. Experiments

In this section, we evaluate the proposed HEMS with real-world data [1], which includes real consumption and PV generation data for different users. The proposed BNN-based NILM is firstly compared with other state-of-the-art models. Based on the NILM results, the robustness and effectiveness of the proposed algorithm for HEMS are evaluated through two different users: one is a prosumer, and the other is a consumer without renewable generators.

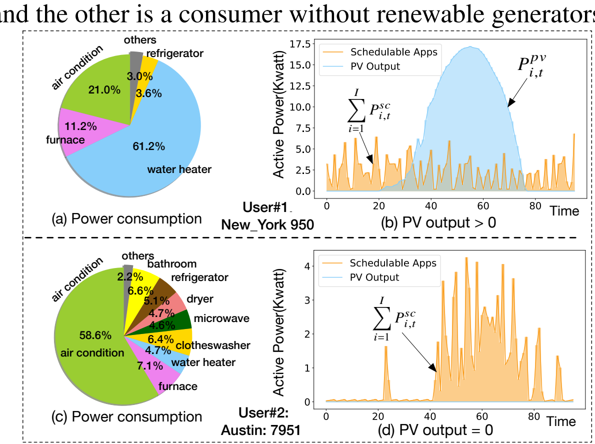

Figure 6: Power consumption behavior of two different consumers. (a) and (c) show the user's power consumption of appliances for a month. (b) and (d) show the power consumption of the schedulable appliances and PV output in one day with 15-minute time interval.

4.1. Dataset

Dataport is the world's largest resource for residential energy use data and is designed to support research in addressing climate crisis. It provides access to static time-series data for 75 homes from New York, California, and Austin. In this work, the performance of the NILM is evaluated with the 1-minute data collected for six months. Two different real-world users with quite different power consumption behaviors are adopted to evaluate the effectiveness of our proposed algorithm. User #1 is a prosumer with PV panels in New York, while user #2 is a consumer without PV panels in Austin. As shown in Fig. 6, the power consumption habits of different users vary considerably. In this work, six different appliances, which are the air conditioning (AC), the furnace (FN), the water heater (WH), the dishwasher (DW), the clothes washer (CW), and the dryer (DY) are regarded as the schedulable appliances.

4.2. Experimental Settings

1) Implementation Details: For the NILM, the raw data is firstly preprocessed for missing values by splitting the sequence into subsequences when the duration is less than 5 minutes. Then, a sliding window $L = 60$ runs over the data with a step size to obtain a sample $\boldsymbol{x} = (x_1, \dots, x_L)$ and its corresponding label $\boldsymbol{y}^i = (y^i_{L-T_y}, \dots, y^i_L)$, where

[1] https://www.pecanstreet.org/dataport/

Table 1
Results NILM for different users. u_i^{nilm} is the mean uncertainty

Metrics	Model	User #1					User #2					
		AC	WH	FN	CW	DY	AC	WH	FN	DW	CW	DY
SAE (Watt)	Seq2Seq [33]	123.6	207.52	53.54	109	23.65	59.51	28.06	29.57	16.21	31.97	68.17
	SCA [34]	88.56	211.27	57.13	21.99	21.38	50.97	20.04	27.34	18.79	32.21	59.87
	MGRU [39]	63.53	130.24	95.81	23.5	19.53	54.09	26.43	27.91	19.57	32.05	55.85
	bSeq2Seq	130.83	161.82	43.47	94.29	22.31	65.02	22.57	29.63	**14.11**	35.66	68.23
	Ours	**61.01**	**109.68**	**41.21**	**19.43**	18.54	**44.28**	**17.26**	**24.88**	16.74	**31.11**	**43.89**
f_1(%)	Seq2Seq [33]	77.76	86.58	62.68	0.00	0.00	93.08	66.67	**83.88**	9.45	82.11	41.17
	SCA [34]	68.24	15.16	13.99	0.00	0.00	59.53	67.5	13.32	27.62	79.63	34.85
	MGRU [39]	93.7	88.77	35.57	0.00	0.00	90.12	65.82	63.8	25.17	75.25	35.99
	bSeq2Seq	69.79	89.12	**65.2**	0.00	0.00	92.25	72.78	81.47	11.48	81.16	33.36
	Ours	**95.91**	**96.57**	63.28	**0.00**	0.00	**94.4**	**81.97**	83.24	**41.76**	**83.98**	**43.84**
u_i^{nilm}	bSeq2Seq	0.079	0.0404	**0.0967**	**0.068**	0.6421	0.282	0.0621	**0.057**	0.2928	0.07	0.2091
	Ours	**0.0557**	**0.0338**	0.2407	0.1119	**0.4528**	**0.207**	**0.0561**	0.0916	**0.2606**	**0.0489**	**0.2599**

we set $T_y = 10$. One-week historical data $K = 7$ of user #1 and user #2 are used for testing the performance of the proposed NILM model. For user #1 with PV, the BESS's capacity is set as $E_{bess}^{max} = 5.7$ kWh with the rated SoC range [10%, 90%]. The maximum charging/discharging power of the BESS are $P_t^{ch} = 2.5$ and $P_t^{dc} = 2.0$ kW with the charging/discharging efficiency 0.82/1.04. To obtain the *on/off* state of the appliance, a threshold $\xi_i = 50$ watts is adopted. For the HEMS optimization model, one day is divided into $T = 96$ time slots and each time slot includes $T_r = 15$ minutes. The reward of the DR event is $\lambda = 10$ cents/kWh. In this paper, the peak points that are larger than half of POT and PTI's maximum values are used to calculate the extended POT and PTI according to the Equation (22) and Equation (24) for the optimization. The NILM experiments are conducted on one GTXGeforce 1080Ti GPU with Pytorch, and the Gurobi solver is used for the optimization task.

2) Comparison Models for NILM: Four models for comparison studies are constructed to investigate the effectiveness and superiority of our proposed BNN-enabled NILM. Sequence to sequence (**Seq2Seq**) proposed in [33] is regarded as the benchmark. **SCA** [34] and **MGRU** [39] are two of the state-of-the-art methods that disaggregate energy from the total power with multi-task learning. To compare the traditional neural network with the Bayesian neural network, Bayesian is also applied to the Seq2Seq architecture referred here as **bSeq2Seq** model.

3) Evaluation Metrics of NILM: The performances of NILM are evaluated with signal aggregate error (SAE) and f_1 score, which are the most widely adopted metrics for NILM study [34, 39, 46],

$$\mathrm{SAE} = \frac{1}{N_a}\sum_{n=1}^{N_a}\frac{1}{T_\delta}\left|\sum_{t=1}^{T_\delta}\hat{y}_{i,t} - \sum_{t=1}^{T_\delta}y_{i,t}\right| \tag{51}$$

$$f_1 = \frac{2 \times precision \times recall}{precision + recall} \tag{52}$$

$$precision = \frac{TP}{TP+FP}, \quad recall = \frac{TP}{TP+FN} \tag{53}$$

where T_δ is the number of time steps in a time period δ, such as one hour. We set T_δ to 60, which corresponds to the number of data points in an hour with a 1-minute sampling frequency. TP, FP, FN are the true positive, false positive and false negative, respectively.

4.3. Results and Discussions of NILM

Case 1: NILM results. As can be seen from Table I, our proposed model outperforms other methods, especially for air conditioning, water heater, and cloth washer. Without using cloth washer and dryer for user #1 in the test data, the f_1 is zero and SAE is larger than zero means there are false positive points (see Fig. 7 (d)). Compared with the results of Seq2Seq and bSeq2Seq, although BNN increases the model complexity, it does not compromise NILM's performance. Specifically, BNN performs better than the traditional neural network for the water heater, which has larger power consumption when they are *on* (see Fig. 7 (b)). For the furnace with very small active power consumption, the most simple architecture model, Seq2Seq, achieved relative higher accuracy for *on/off* state detection. Compared with the bSeq2Seq model, the proposed model achieves smaller uncertainties for the air conditioning, the water heater, the dishwasher, and the dryer. The smaller SAE for energy disaggregation or the higher f_1 score for *on/off* state detection does not mean the smaller uncertainty score of the results.

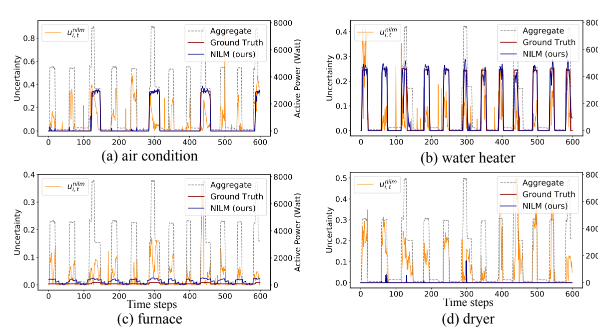

Figure 7: Disaggregation results of different appliances for user #1. The uncertainty of each time step has been plotted.

Case 2: Calculation of preference level. According to the definitions discussed in Section II and Section III, the energy consumption behaviors and the preference levels of different users can be quantitatively evaluated with their different levels of uncertainty. Fig. 8 shows the maximum operation time and the maximum operation number of different appliances for different users with the ground truth data and the NILM results. The disaggregated operation time for the furnace in user #1 and the dryer in user #2 deviate from the ground truth with a relatively bigger uncertainty. For other appliances, the results from our proposed

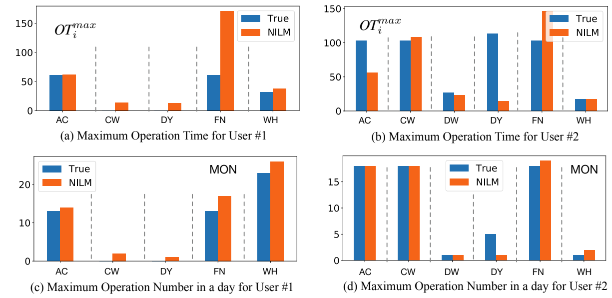

Figure 8: Comparison of the maximum operation time and operation number with ground truth data and the NILM results.

model can achieve high accuracy for maximum operation time and maximum operation number.

The POT and PTI of different appliances for user #2 are further presented in Fig. 9. It can be seen that the results with our proposed model can follow the actual energy consumption behavior habits of the users. It is also observed that even for the same appliance, the usage habits of different users are completely different (see Fig. 9 (a) and (c)), which also illustrates the necessity of considering user behavior effects in HEMS. As shown in Fig. 9 (b) and (d), both the preferred operation time and preferred operating temperature can be identified with our proposed algorithm.

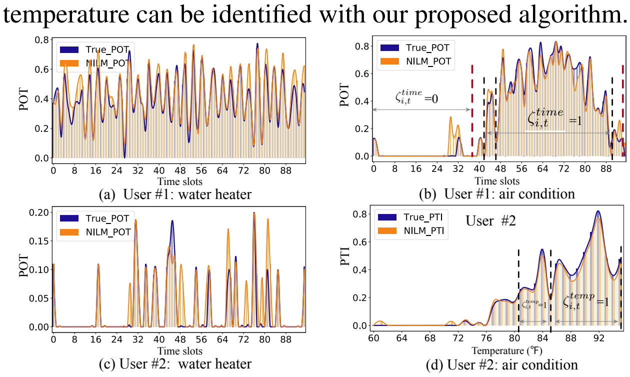

Figure 9: Comparison of the user behavior calculated with the ground truth data and the NILM results.

Case 3: Uncertainty score. The uncertainty score of the NILM results for the case shown in Fig. 9(c) are visualized in Fig. 10. With the Bayesian algorithm, the NILM result is just one of the various outcome possibilities of the model. This is the first study to consider the uncertainty score of the neural network for NILM in HEMS for the electrical appliances scheduling.

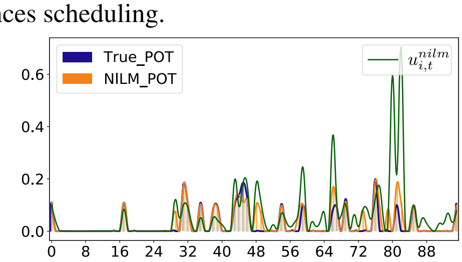

Figure 10: The POT and uncertainty of the water heater in user #2.

4.4. Day-Ahead Home Energy Management

The HEMS optimization experiments are conducted with the actual energy consumption data and NILM results for the prosumer and the consumer. Note that the DR event signals are set to zero in case study 4 and case study 5.

Case 4: HEMS for a prosumer with renewable generators:

As shown in Fig.6 (b), user #1 has a renewable generator, which reaches about 17 KWatts in peak time and can be used for home energy consumption or selling to the grid. With the TOU price and spot price signals shown in Fig. 11(a), the objective function in Equation (29) can be optimized. Fig. 11 (b) shows the performance of the traditional HEMS and the proposed NILM-based HEMS with the actual power consumption data and the NILM results data. The traditional HEMS operates for only minimizing energy cost $\mathcal{C}$ without considering the consumer's preference level $\mathcal{P}$. As the excess energy can be sold to the grid, the prosumer earns about \$14 with the traditional HEMS, which has more profit but low-level preference without considering the preference level $\mathcal{P}$ in the optimization model. In contrast, the proposed algorithm increases the cost, however, with a much higher preference level. Compared with the traditional HEMS, the proposed NILM-based HEMS sacrifices 35.09% of the electricity cost to increase the preference level by three times for the prosumer.

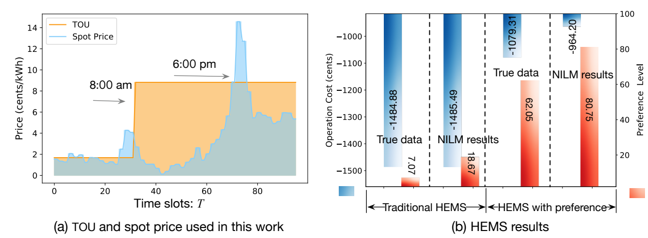

Figure 11: Prices and the comparison of the proposed algorithm with the traditional HEMS for user #1 with renewable generators.

In Fig. 11 (b), it is also observed that the HEMS results with the NILM data coincide perfectly alongside the results with the actual energy consumption data. The NILM-based HEMS achieves a relatively smaller cost and comparable preference level than the true data-based HEMS. We further show the scheduling of the appliances and the BESS in Fig. 12. It can be seen that although the estimated dryer and furnace have a larger active power than the true values, the developed model generates a very similar scheduling time as the model using the true appliance energy consumption values. Especially for the furnace, the f_1 score for the *on/off* states detection is not high enough with 63.28%; however, the HEMS is robust enough with the NILM error by introducing uncertainty in the optimization model. Similar scheduling results in Fig. 12 (b) and (d) based on the true data and NILM outputs respectively illustrate the strong robustness of our proposed algorithm. It is clear that when the PV output is reasonably large enough at midday, the user can sell the surplus PV output to the grid.

Case 5: HEMS for a consumer without renewable generators: While designing HEMS for the prosumers, the degree of consumer participation in DR also should be considered. The research for achieving reductions in both energy consumption and carbon emissions through active participation in DR from consumers with no renewable

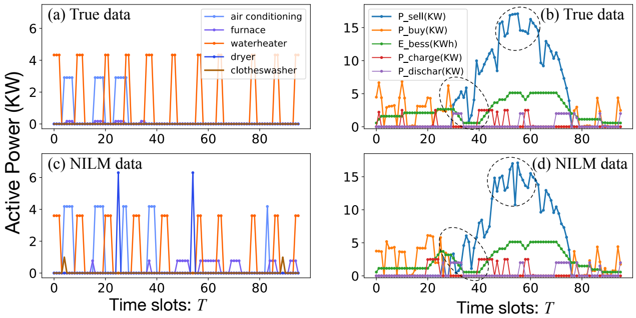

Figure 12: Comparison of the scheduling results of user #1 with the ground truth data and the NILM results.

generators has not been studied before. In this case, user #2 shown in Fig. 6 (c) and (d) is used to evaluate our proposed algorithm further. Note that we made a reasonable assumption that the consumer without renewable generators has no battery energy storage system. However, the proposed model is also applicable to those consumers who have batteries installed but have no renewable generators.

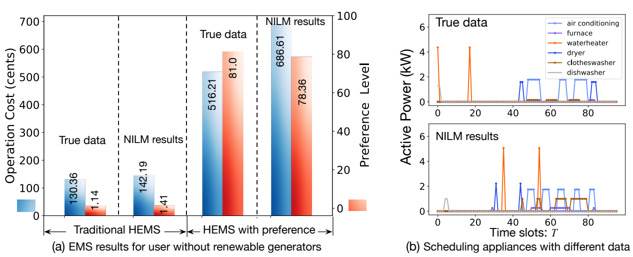

Figure 13: Comparison of the HEMS results and the scheduling results for different schedulable appliances with ground truth data and the NILM results.

As can be seen from Fig. 13 (a), even though the traditional algorithm decreases the consumer's energy cost, it also severely reduces the consumer's preference level. Although the *on/off* state detection results for user #2 (shown in Table 1) do not show high accuracy enough, especially for the dishwasher and the dryer, the HEMS results with true data show a similar pattern as the NILM associated results. With the proposed NILM-based HEMS, the cost with NILM results has only increased by 33.0%, but the preference level shows little difference compared to the results from the actual energy consumption record (and the use of real record is normally not feasible in the real-life scenario). Hence the practical meaning of the NILM-based HEMS is assured. This further articulates the robustness of our proposed algorithm. Fig. 13 (b) shows that the scheduling time for different appliances with different data is very similar, which further demonstrates the effectiveness of our proposed HEMS with the NILM results.

Case 6: DR event: The proposed HEMS can receive the DR signals from the utility during peak times. We set three DR signals at different times in this case study. The user receives the DR signals for increasing ($\gamma = 1$) or decreasing ($\gamma = -1$) the power consumption at peak time. Fig.14 (a) shows the HEMS results of the traditional algorithm and the proposed algorithm supported by the NILM outputs. First, compared to the traditional method, the proposed method can keep a relatively higher preference level while sacrificing some energy cost. With the innovative introduction of the user's preference level to the DR reward, the proposed algorithm with DR event consideration benefits both the profit and customer preference level and can reduce the energy cost while maintaining a comparable or better preference level. From Fig. 14 (b), it can be seen that the HEMS decreases consumer utility costs through better appliance scheduling with more effective DR events participation. Furthermore, the scheduling results for different appliances demonstrate that, instead of only responding to the DR signals for maximum rewards, the proposed HEMS favors scheduling appliances through a better trade-off between the rewards gained from DR events and the user preference level achievement. The same conclusions can also be drawn from the results of the prosumer shown in Fig. 15.

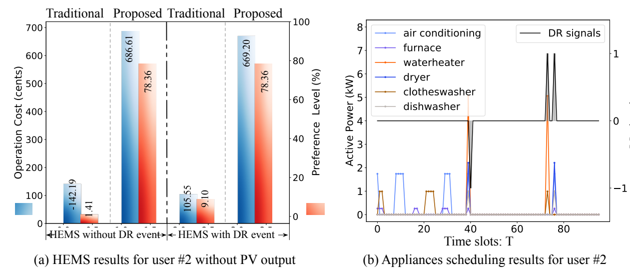

Figure 14: Comparison of the HEMS results with DR events for user #2 without renewable generators.

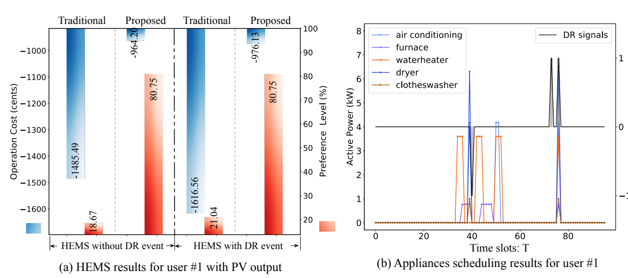

Figure 15: Comparison of the HEMS results with DR events for user #1 with renewable generator.

Case 7: The effect of priority for the alternative objective. The main challenge facing multiple competing objectives is deciding how to manage their trade-offs. With the weighted sum method shown in Eq. (29), the weighted combination of the individual objectives can be solved with a priority for each objective and optimized in priority order. Only the solutions that would not degrade the objective values of higher-priority objectives will be considered when optimizing for one objective. In the above discussions, the preference level has a higher priority than the energy cost, which will minimize the energy cost while ensuring the preference level. In Table 2, four scenarios with two parameters: DR event and Preference, are compared with different priority objectives. If the DR event is false, it means the optimization model does not consider the DR reward. While false preference indicates that the optimization model is the traditional model without considering the user's energy consumption habit.

Table 2
Optimization results of user #2 for different scenarios with different priority objectives.

DR Event	Preference	Priority Preference			Priority Cost		
		C	λP^{dr}	$\mathcal{P}$	C	λP^{dr}	$\mathcal{P}$
False	False	142.19	0.00	1.42	142.19	0.00	1.41
False	True	*686.61*	0.00	**78.36**	142.19	0.00	6.71
True	False	105.55	225.25	9.10	**105.55**	225.25	9.10
True	True	*669.20*	17.41	**78.36**	131.02	52.03	10.56

Table 3
The computational complexity of the models for NILM

Methods	NILM				
	Seq2Seq	SCA	MGRU	bSeq2Seq	Ours
Training time (Min)	**6.82**	19.02	12.92	22.90	25.10
Model size (Mb)	3.12	23.99	**1.52**	12.47	32.07

As shown in Table 2, the optimization results of priority objective P can maximize the preference level with a relatively larger energy cost. When the DR event is considered, the energy cost can be significantly reduced with the traditional model. Because the proposed model introduces preference level to the reward of DR events, the reward is relatively smaller than the results without considering the user's preference level. On the contrary, the energy cost is significantly minimized by setting the energy cost as the priority objective. According to our proposed HEMS model, users can independently choose whether they care more about energy cost or energy consumption habits in their energy management.

Case 8: Analysis of computation complexity for the overall framework. This case compares the computational time and complexity of the proposed model with other models. For the NILM, the washing machine is taken as an example for comparison different networks. The training time and model size are listed in Table 3, in which we can see that the introduction of Bayesian to the network increases not only the model size but also the training time to get a satisfying result with uncertainty.

The computation complexity of the HEMS objective function is analyzed in the Appendix, which is concluded that the complexity is $\mathcal{O}\left(n^{3.5}B\cdot 2^{|\mathcal{I}||\mathcal{T}|}\right)$, where B is the bit size of integer data.

The above case studies demonstrate the effectiveness of the proposed HEMS for both consumers without renewable resources and prosumers with PV. The similar optimization results with ground truth data and the NILM results with a small f_1 score evaluate the robustness of the proposed algorithm. To maintain a relatively high level user preference, the HEMS will sacrifice appropriate savings in energy costs. By introducing the preference level to the DR reward in the optimization model, the proposed HEMS can improve or maintain the user's preference level while responding to the DR signals. Users can customize the priority given to energy cost saving and preference levels keeping with the proposed HEMS.

5. Conclusion

This paper presents a NILM-based HEMS algorithm for residential users that incorporates the uncertainty of data-driven results to achieve the best trade-off between electricity cost and the preference level. The proposed HEMS includes two stages: a quantitative user behavior characterization and an optimization counterpart. In the first stage, the appliance-level energy consumption and *on/off* state detection of the user are monitored with the proposed BNN-enabled NILM. The experiments use real-world datasets to demonstrate that the proposed NILM can achieve relatively high accuracy when uncertainty score are taken into account. With the NILM results, the proposed five metrics for user behavior characterization can quantitatively evaluate the user's energy consumption habits. Additionally, the preference level for appliance scheduling can be provided, resulting in a more specific consumer model in our proposed HEMS.

In the optimization stage, the HEMS optimization results with NILM outputs can perfectly coincide the results with ground truth data for both the prosumer and the consumer. Even for the scenarios that the NILM results of an appliance deviate from its actual record, which is unavoidable in all the data-driven applications, the consideration of uncertainty score in our proposed algorithm can still guarantee the effectiveness of our HEMS. Benchmarked with traditional HEMS, the NILM-based HEMS can balance a better trade-off between the electricity cost and the preference level for the prosumer and consumer. Besides, the proposed HEMS also can respond to the DR event without reducing the user's preference level.

A. Analysis of the computational complexity

To analyze the computational complexity of the HEMS optimization model, i.e., Eqs. (26)-(47), we begin by summarizing the objective function and the constraints, which are as follows:

$$\min_{\Xi} \mathcal{C} = \sum_{t=1}^{T}(\lambda_t^{TOU}P_t^{grid} - \lambda_t^{SP}P_t^{sell} - \lambda_t^{dr}P_t^{dr})\Delta t \quad (26)$$

[-9pt]

$$\begin{aligned}\max_{\Xi} \mathcal{P} &= \sum_{t=1}^{T}\sum_{i=1}^{I}\left[(\mathcal{P}_{i,t}^{time} + \mathcal{P}_{i,t}^{temp})(1-u_{i,t}^{nilm}s_{i,t})\right] \\ &= \sum_{t=1}^{T}\sum_{i=1}^{I}\left[(s_{i,t}\cdot\zeta_{i,t}^{time} + s_{i,t}\cdot\zeta_{i,t}^{temp})(1-u_{i,t}^{nilm}s_{i,t})\right]\end{aligned} \quad (26+)$$

$$\begin{aligned}\min_{\Xi} \mathcal{B} =&(1-\omega)\mathcal{C} + \omega(-\mathcal{P}) \quad (29)\\ =&(1-\psi(\bar{u}))\mathcal{C} + \psi(\bar{u})(-\mathcal{P}) \quad (30)\end{aligned}$$

$$\lambda_{i,t}^{dr} = \begin{cases}\lambda(1-s_{i,t-1})\cdot s_{i,t}\cdot rfou_{i,t}^{start}, \ \gamma = 1\\ \lambda s_{i,t-1}\cdot(1-s_{i,t})\cdot rfou_{i,t}^{end}, \ \gamma = -1\\ 0, \ \gamma = 0\end{cases} \quad (35)$$

$$\lambda_t^{dr}P_t^{dr} = \sum_{i=1}^{I}(\lambda_{i,t}^{dr}\cdot P_{i,t}^{sc}\cdot|\gamma|),\ \forall t\in\mathcal{T} \quad (36)$$

where $(s_{i,t}, P_t^{grid}, P_t^{sell}, \lambda_t^{dr}, P_t^{dr}, P_t^{ch}, P_t^{dc})$ are the decision variables.

s.t.

$$P_t^{grid} - P_t^{sell} + P_t^{pv} - P_t^{ch} + P_t^{dc} - P_t^{app} = 0 \quad (38)$$

$$P_t^{app} = \sum_{h=1}^{H_{ns}} P_{h,t}^{nsc} + \sum_{i=1}^{I} P_{i,t}^{sc} \cdot s_{i,t},\ \forall t \in \mathcal{T} \quad (39)$$

$$0 \le P_t^{sell} \le (P_t^{pv} + P_t^{dc})(1 - \delta_t^{grid}),\ \forall t \in \mathcal{T} \quad (40)$$

$$0 \le P_t^{grid} \le P_{max}^{grid} \delta_t^{grid},\ \forall t \in \mathcal{T} \quad (41)$$

$$s_{i,t}, \delta_t^{grid} \in \{0,1\},\ \forall i \in \mathcal{I},\ \forall t \in \mathcal{T} \quad (42)$$

$$SoC_{t+1} = SoC_t + (P_t^{ch}\eta_t^c - P_t^{dc}/\eta_t^{dc})\Delta t / E_{bess}^{max} \quad (43)$$

$$SoC^{min} \le SoC_t \le SoC^{max},\ \forall t \in \mathcal{T} \quad (44)$$

$$0 \le P_t^{ch} \le P_{ch,t}^{max} \delta_t^{ch},\ \forall t \in \mathcal{T} \quad (45)$$

$$0 \le P_t^{dc} \le P_{dc,t}^{max}(1 - \delta_t^{ch}),\ \forall t \in \mathcal{T} \quad (46)$$

$$\delta_t^{ch} \in \{0,1\}, \forall t \in \mathcal{T}. \quad (47)$$

First, we reduce the HEMS model into a simplified one by fixing the continuous decision variables P_t^{grid}, P_t^{sell}, P_t^{dr}, λ_t^{dr}, P_t^{ch} and P_t^{dc}. The reduced version is as follows.

$$\min_{s} \bar{\mathcal{C}} = -\sum_{t=1}^{T} (\lambda_t^{dr} P_t^{dr}) \Delta t \quad (54)$$

$$\max_{s} \bar{\mathcal{P}} = \sum_{t=1}^{T} \sum_{i=1}^{I} \left\{ (s_{i,t} \cdot \zeta_{i,t}^{time} + s_{i,t} \cdot \zeta_{i,t}^{temp})(1 - u_{i,t}^{nilm} s_{i,t}) \right\} \quad (55)$$

$$\min_{s} \bar{\mathcal{B}} = (1-\omega)\bar{\mathcal{C}} + \omega(-\bar{\mathcal{P}}) eq : sof \quad (56)$$

s.t.

$$\text{Eqs.}(35) - (36), \quad (57)$$

$$s_{i,t} \in \{0,1\},\ \forall i \in \mathcal{I},\ \forall t \in \mathcal{T}. \quad (42)$$

The reduced formulation is a quadratically constrained quadratic programming (QCQP) model if removing binary restrictions of $s_{i,t}$. According to [53], the general QCQP is already NP-hard. If adding the binary constraints of $s_{i,t}$, the model becomes a mixed integer quadratically constrained quadratic programming (MIQCQP), which is much harder than continuous QCQP. Therefore, the entire version of the HEMS model is also NP-hard.

Then, if fixing the decision variables $s_{i,t}$, the objective function $\mathcal{B}$ and the constraints can be simplified as follows,

$$\min_{\boldsymbol{P}^{sell}, \boldsymbol{P}^{grid}, \boldsymbol{P}^{ch}, \boldsymbol{P}^{dc}} \underline{\mathcal{C}} = \sum_{t=1}^{T} (\lambda_t^{TOU} P_t^{grid} - \lambda_t^{SP} P_t^{sell}) \Delta t \quad (58)$$

[-9pt]

$$\min_{\boldsymbol{P}^{sell}, \boldsymbol{P}^{grid}, \boldsymbol{P}^{ch}, \boldsymbol{P}^{dc}} \underline{\mathcal{B}} = \underline{\mathcal{C}} \quad (59)$$

where $\underline{\mathcal{B}}$ is a reduction of $\mathcal{B}$. Note that Eqs. TeXFolio:eq40, TeXFolio:eq41, TeXFolio:eq45, and TeXFolio:eq46 contain nonlinear terms. Those non-linear items can be equivalently linearized by introducing big-$\boldsymbol{M}$ constraints and corresponding auxiliary variables, leading to the reduced model a linear programming. According to [54], the general linear programming can be solved in time $\mathcal{O}(n^{3.5}B)$, where B is the bit size of integer data. However, the complexity will increase exponentially if we consider $s_{i,t}$ as binary decision variables. More specifically, the overall complexity is $\mathcal{O}\left(n^{3.5}B \cdot 2^{|\mathcal{I}||\mathcal{T}|}\right)$. Based on the above discussion, the HEMS model is NP-hard.

References

[1] P. Nejat, F. Jomehzadeh, M. M. Taheri, M. Gohari, M. Z. Abd. Majid, A global review of energy consumption, CO2 emissions and policy in the residential sector (with an overview of the top ten CO2 emitting countries), Renewable and Sustainable Energy Reviews 43 (2015) 843–862.

[2] C. E. Council, Energy security board: moving to a two-sided market, COAG Energy Council (2020).

[3] M. Karami, R. Madlener, Business models for peer-to-peer energy trading in germany based on households' beliefs and preferences, Applied Energy 306 (2022) 118053.

[4] R. Markovič, M. Gosak, V. Grubelnik, M. Marhl, P. Virtič, Data-driven classification of residential energy consumption patterns by means of functional connectivity networks, Applied Energy 242 (2019) 506–515.

[5] S. Barja-Martinez, F. Rücker, M. Aragüés-Peñalba, R. Villafafila-Robles, Munné-Collado, P. Lloret-Gallego, A novel hybrid home energy management system considering electricity cost and greenhouse gas emissions minimization, IEEE Transactions on Industry Applications 57 (3) (2021) 2782–2790.

[6] Y. Deng, Y. Zhang, F. Luo, G. Ranzi, A many-objective hems with multi-scale occupant satisfaction modelling and second-life bess utilization, IEEE Transactions on Sustainable Energy (2022) 1–1.

[7] Z. Wang, U. Munawar, R. Paranjape, Stochastic optimization for residential demand response with unit commitment and time of use, IEEE Transactions on Industry Applications 57 (2) (2021) 1767–1778.

[8] R. R. Avula, J.-X. Chin, T. J. Oechtering, G. Hug, D. Månsson, Design framework for privacy-aware demand-side management with realistic energy storage model, IEEE Transactions on Smart Grid 12 (4) (2021) 3503–3513.

[9] Z. Pang, Y. Chen, J. Zhang, Z. O'Neill, H. Cheng, B. Dong, How much hvac energy could be saved from the occupant-centric smart home thermostat: A nationwide simulation study, Applied Energy 283 (2021) 116251.

[10] O. Alrumayh, K. Bhattacharya, Flexibility of residential loads for demand response provisions in smart grid, IEEE Transactions on Smart Grid 10 (6) (2019) 6284–6297.

[11] P. Munankarmi, J. Maguire, S. P. Balamurugan, M. Blonsky, D. Roberts, X. Jin, Community-scale interaction of energy efficiency and demand flexibility in residential buildings, Applied Energy 298 (2021) 117149.

[12] Z. Zhang, Y. Huang, Q. Huang, W.-J. Lee, A novel hierarchical demand response strategy for residential microgrid with time-varying price, in: 2020 IEEE Industry Applications Society Annual Meeting, 2020, pp. 1–8.

[13] Y. Du, F. Li, Intelligent multi-microgrid energy management based on deep neural network and model-free reinforcement learning, IEEE Transactions on Smart Grid 11 (2) (2020) 1066–1076.

[14] S. Gao, C. Xiang, M. Yu, K. T. Tan, T. H. Lee, Online optimal power scheduling of a microgrid via imitation learning, IEEE Transactions on Smart Grid 13 (2) (2022) 861–876.

[15] D. Qiu, Z. Dong, X. Zhang, Y. Wang, G. Strbac, Safe reinforcement learning for real-time automatic control in a smart energy-hub, Applied Energy 309 (2022) 118403.

[16] M. Yousefi, A. Hajizadeh, M. N. Soltani, B. Hredzak, Predictive home energy management system with photovoltaic array, heat pump, and plug-in electric vehicle, IEEE Transactions on Industrial Informatics 17 (1) (2021) 430–440.

[17] M. Killian, M. Zauner, M. Kozek, Comprehensive smart home energy management system using mixed-integer quadratic-programming, Applied Energy 222 (2018) 662–672.

[18] F. Luo, W. Kong, G. Ranzi, Z. Y. Dong, Optimal home energy management system with demand charge tariff and appliance operational dependencies, IEEE Transactions on Smart Grid 11 (1) (2020) 4–14.

[19] Y. Kim, Optimal price based demand response of hvac systems in multizone office buildings considering thermal preferences of individual occupants buildings, IEEE Transactions on Industrial Informatics 14 (11) (2018) 5060–5073.

[20] K. Kwon, S. Lee, S. Kim, Ai-based home energy management system considering energy efficiency and resident satisfaction, IEEE Internet of Things Journal (2021) 1–1.

[21] V. Pilloni, A. Floris, A. Meloni, L. Atzori, Smart home energy management including renewable sources: A qoe-driven approach, IEEE Transactions on Smart Grid 9 (3) (2018) 2006–2018.

[22] M. Afzalan, F. Jazizadeh, Residential loads flexibility potential for demand response using energy consumption patterns and user segments, Applied Energy 254 (2019) 113693.

[23] C. Zhang, S. Lasaulce, L. Wang, L. Saludjian, H. V. Poor, A refined consumer behavior model for energy systems: Application to the pricing and energy-efficiency problems, Applied Energy 308 (2022) 118239.

[24] I. Varlamis, C. Sardianos, C. Chronis, G. Dimitrakopoulos, Y. Himeur, A. Alsalemi, F. Bensaali, A. Amira, Smart fusion of sensor data and human feedback for personalized energy-saving recommendations, Applied Energy 305 (2022) 117775.

[25] F. Alfaverh, M. Denaï, Y. Sun, Demand response strategy based on reinforcement learning and fuzzy reasoning for home energy management, IEEE Access 8 (2020) 39310–39321.

[26] K. Matsui, H. Ochiai, Y. Yamagata, Feedback on electricity usage for home energy management: A social experiment in a local village of cold region, Applied Energy 120 (2014) 159–168.

[27] M. B. Anwar, M. O'Malley, Strategic participation of residential thermal demand response in energy and capacity markets, IEEE Transactions on Smart Grid 12 (4) (2021) 3070–3085.

[28] L. Langer, T. Volling, An optimal home energy management system for modulating heat pumps and photovoltaic systems, Applied Energy 278 (2020) 115661.

[29] H. R. Rocha, I. H. Honorato, R. Fiorotti, W. C. Celeste, L. J. Silvestre, J. A. Silva, An artificial intelligence based scheduling algorithm for demand-side energy management in smart homes, Applied Energy 282 (2021) 116145.

[30] Z. Zheng, Z. Sun, J. Pan, X. Luo, An integrated smart home energy management model based on a pyramid taxonomy for residential houses with photovoltaic-battery systems, Applied Energy 298 (2021) 117159.

[31] S. Shahzad, J. K. Calautit, B. R. Hughes, B. Satish, H. B. Rijal, Patterns of thermal preference and visual thermal landscaping model in the workplace, Applied Energy 255 (2019) 113674.

[32] Y. Himeur, K. Ghanem, A. Alsalemi, F. Bensaali, A. Amira, Artificial intelligence based anomaly detection of energy consumption in buildings: A review, current trends and new perspectives, Applied Energy 287 (2021) 116601.

[33] C. Zhang, M. Zhong, Z. Wang, N. Goddard, C. Sutton, Sequence-to-Point Learning with Neural Networks for Non-Intrusive Load Monitoring, in: The Thirty-Second AAAI Conference on Artificial Intelligence (AAAI-18), 2018.

[34] K. Chen, Y. Zhang, Q. Wang, J. Hu, H. Fan, J. He, Scale- and context-aware convolutional non-intrusive load monitoring, IEEE Transactions on Power Systems 35 (3) (2020) 2362–2373.

[35] Y. Liu, L. Zhong, J. Qiu, J. Lu, W. Wang, Unsupervised domain adaptation for nonintrusive load monitoring via adversarial and joint adaptation network, IEEE Transactions on Industrial Informatics 18 (1) (2022) 266–277.

[36] Y. Yang, J. Zhong, W. Li, T. A. Gulliver, S. Li, Semisupervised multilabel deep learning based nonintrusive load monitoring in smart grids, IEEE Transactions on Industrial Informatics 16 (11) (2020) 6892–6902.

[37] Y. Liu, W. Liu, Y. Shen, X. Zhao, S. Gao, Toward smart energy user: Real time non-intrusive load monitoring with simultaneous switching operations, Applied Energy 287 (2021) 116616.

[38] A. Samadi, H. Saidi, M. A. Latify, M. Mahdavi, Home energy management system based on task classification and the resident's requirements, International Journal of Electrical Power & Energy Systems 118 (2020) 105815.

[39] H. Çimen, N. Çetinkaya, J. C. Vasquez, J. M. Guerrero, A microgrid energy management system based on non-intrusive load monitoring via multitask learning, IEEE Transactions on Smart Grid 12 (2) (2021) 977–987.

[40] H. Mansy, S. Kwon, Optimal hvac control for demand response via chance-constrained two-stage stochastic program, IEEE Transactions on Smart Grid 12 (3) (2021) 2188–2200.

[41] J. Song, Y. Lee, E. Hwang, Time–frequency mask estimation based on deep neural network for flexible load disaggregation in buildings, IEEE Transactions on Smart Grid 12 (4) (2021) 3242–3251.

[42] A. Rafati, H. R. Shaker, S. Ghahghahzadeh, Fault detection and efficiency assessment for hvac systems using non-intrusive load monitoring: A review, Energies 15 (1) (2022).

[43] Y.-H. Lin, M.-S. Tsai, An advanced home energy management system facilitated by nonintrusive load monitoring with automated multiobjective power scheduling, IEEE Transactions on Smart Grid 6 (4) (2015) 1839–1851.

[44] H. Çimen, N. Bazmohammadi, A. Lashab, Y. Terriche, J. C. Vasquez, J. M. Guerrero, An online energy management system for ac/dc residential microgrids supported by non-intrusive load monitoring, Applied Energy 307 (2022) 118136.

[45] K. Chen, Y. Zhang, Q. Wang, J. Hu, H. Fan, J. He, Scale- and context-aware convolutional non-intrusive load monitoring, IEEE Transactions on Power Systems 35 (3) (2020) 2362–2373.

[46] M. D'Incecco, S. Squartini, M. Zhong, Transfer learning for non-intrusive load monitoring, IEEE Transactions on Smart Grid 11 (2) (2020) 1419–1429.

[47] C. Blundell, J. Cornebise, K. Kavukcuoglu, D. Wierstra, Weight uncertainty in neural network, in: Proceedings of the 32nd International Conference on Machine Learning, Vol. 37 of Proceedings of Machine Learning Research, PMLR, Lille, France, 2015, pp. 1613–1622.

[48] K. He, X. Zhang, S. Ren, J. Sun, Deep residual learning for image recognition, 2016 IEEE Conference on Computer Vision and Pattern Recognition (CVPR) (2016) 770–778.

[49] M. Bayes, M. Price, An essay towards solving a problem in the doctrine of chances. by the late rev. mr. bayes, f. r. s. communicated by mr. price, in a letter to john canton, a. m. f. r. s., Philosophical Transactions (1683-1775) 53 (1763) 370–418.

[50] S. Messaoud, A. Bradai, E. Moulay, Online gmm clustering and mini-batch gradient descent based optimization for industrial iot 4.0, IEEE Transactions on Industrial Informatics 16 (2) (2020) 1427–1435.

[51] R. Marler, J. Arora, The weighted sum method for multi-objective optimization: new insights, Structural and Multidisciplinary Optimization 41 (2010) 853–862.

[52] M. Hamidi, A. Raihani, M. Youssfi, O. Bouattane, A new modular nanogrid energy management system based on multi-agent architecture, International Journal of Power Electronics and Drive Systems (IJPEDS) 13 (1) (2022) 178–190.

[53] S. A. Vavasis, Quadratic programming is in np, Information Processing Letters 36 (2) (1990) 73–77.

[54] N. Karmarkar, A new polynomial-time algorithm for linear programming, in: Proceedings of the sixteenth annual ACM symposium on Theory of computing, 1984, pp. 302–311.